Supporting Information

Furukawa et al. 10.1073/pnas.1312649110

SI Materials and Methods

We amplified the nucleotide sequences corresponding to residues 74–219 of Mincle (macrophage inducible C-type lectin) and residues 61–215 of MCL (macrophage C-type lectin) using the following primer sets: 5′-GAGATATACATATGGGTTCAGTCAAGAATT-3′ and 5′-AGAGGATTCTTAAAGAGATTTTCCTTTGTT-3′ (for Mincle; restriction sites are underlined) and 5′-GAGATATACATATGCATGCAAAGCTCAAAT-3′ and 5′-AGAGGATTCGTTCAATGTTGTTCCAGGTATTTT-3′ (for MCL; restriction sites are underlined), and human PBMC cDNA as a template. PCR-amplified Mincle and MCL products were digested with BamHI/NdeI and ligated into BamHI/NdeI-digested pET22 (Novagen) to produce pET22-Mincle and pET22-MCL, respectively.

The construction of the plasmid to express the I99K mutant is described below. Initially, two fragments, the T7 promoter to the mutant point and the mutant point to the T7 terminator, were amplified by the primer sets 5′-TAATACGACTCACTATAG-3′ and 5′-GGTGTCAGTAGAAAAGAAGTAGCAG-3′, and 5′-AAATCCTGGGCGTTAAGTTTAAAGA-3′ and 5′-CCGCTGAGCAATAACTAGC-3′, using pET22-Mincle, respectively (mutation site is underlined). The entire mutated Mincle fragment was amplified by PCR from the fragments of the T7 promoter to the mutant point and the mutant point to the T7 terminator with the primer sets 5′-TAATACGACTCACTATAG-3′ and 5′-CCGCTGAGCAATAACTAGC-3′. The amplified entire mutated Mincle PCR product was digested with BamHI/NdeI and ligated into BamHI/NdeI-digested pET22 to produce pET22-hMincle I99K.

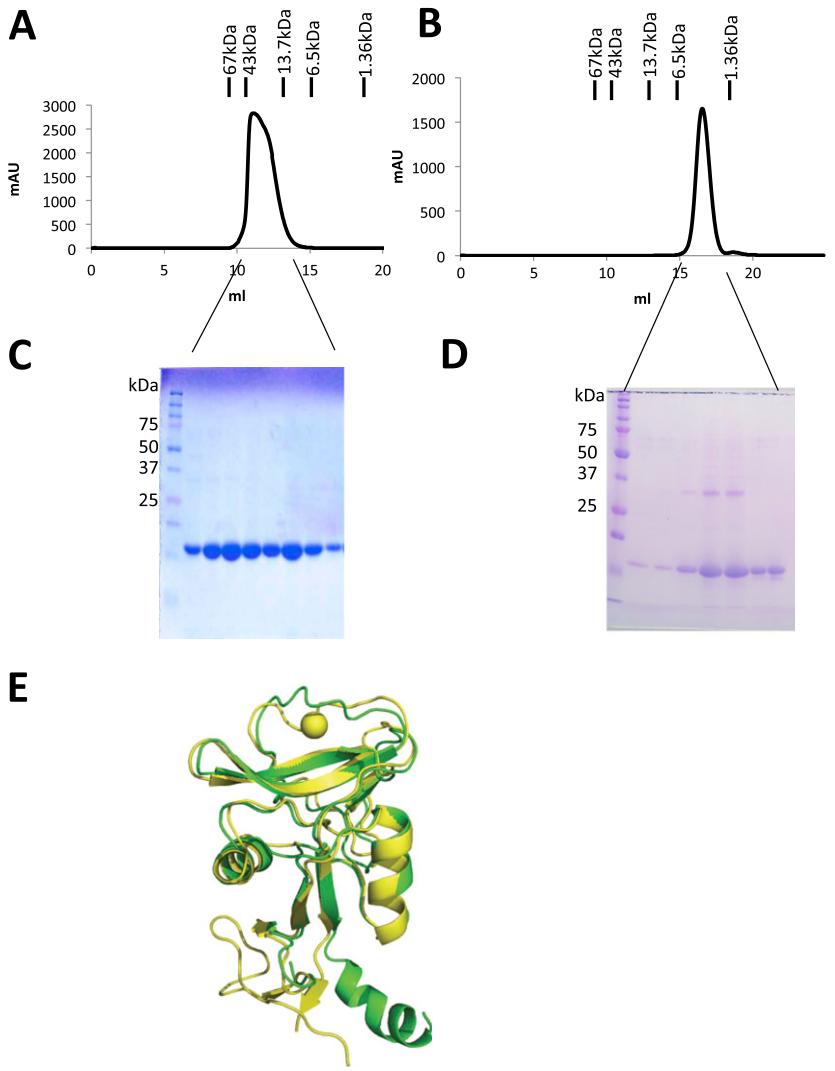

Fig. S1. Elution profiles of MCL (*A*) and Mincle (*B*) from size-exclusion chromatography using a Superdex 75 10/300 GL column (GE Healthcare) are shown. The eluted fractions of MCL (*C*) and Mincle (*D*) were separated and stained by Coomassie brilliant blue. (*E*) The superimposition of crystal (yellow) and solution (PDB ID code 2LS8) (green) structures of MCL is shown. Spheres indicate Ca^{2+} ions. AU, arbitrary unit.

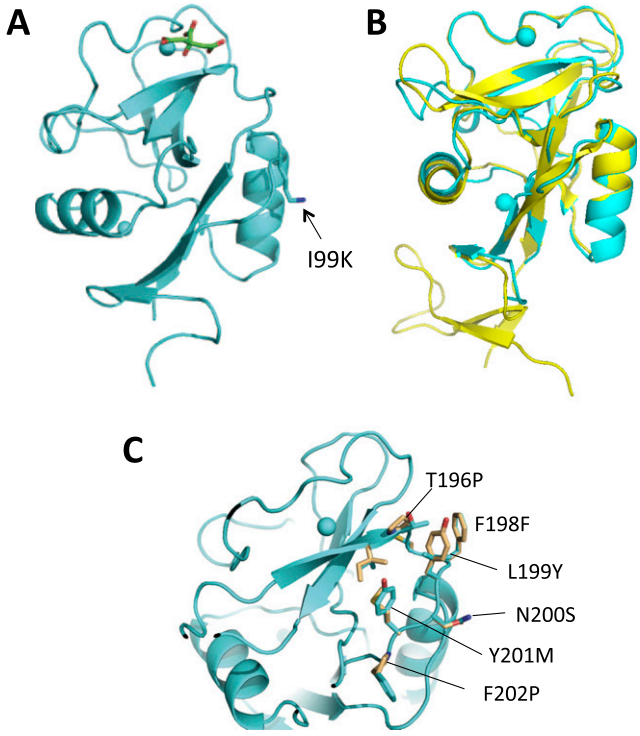

	human	mouse	solvent-accessible surface(Å^2)
195	Val	Ile	5.7
196	Thr	Pro	35.3
197	Cys	Cys	3
198	Phe	Phe	155.8
199	Leu	Tyr	78.1
200	Asn	Ser	102.6
201	Tyr	Met	47
202	Phe	Pro	32.6
203	Arg	Trp	5.7

Fig. S2. Crystal structures of MCL and Mincle. (*A*) A stick model of lysine mutated from isoleucine at residue 99 of Mincle is shown in a cartoon model of Mincle. (*B*) The superimposed structures of MCL (yellow) and Mincle (cyan) are shown. Spheres indicate Ca^{2+} ions. (*C*) Amino acid substitutions on the hydrophobic patch between human and mouse Mincle are mapped onto the crystal structure together with their solvent-accessible areas. The area sizes of solvent-accessible surface of each residue in the putative hydrophobic loops are shown in the table. The sizes were calculated by the AREAIMOL program in CCP4 (www.ccp4.ac.uk).

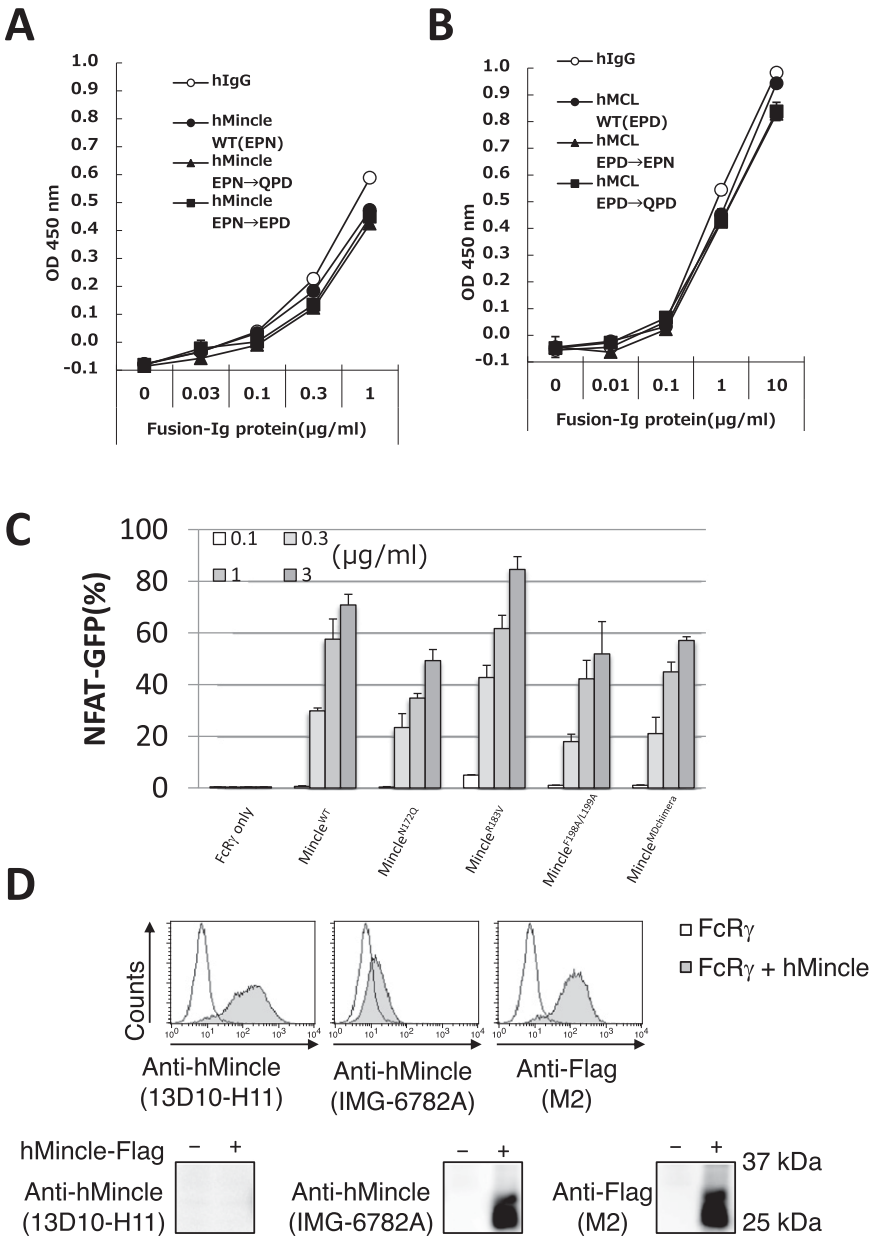

Fig. S3. Control experiments of Figs. 3 and 4. In vitro binding assay of Mincle and MCL mutants and reporter cell assay of Mincle mutants. (*A* and *B*) Mincle–Ig, mutated Mincle–Ig, or human (h)IgG (*A*) and MCL–Ig, mutated MCL–Ig, or hIgG (*B*) were incubated with plate-coated anti-IgG antibody. The bound proteins were detected by anti–hIgG-HRP. (*C*) Reporter cells expressing Mincle or its mutants were stimulated with an anti-Mincle antibody, 13D10-H11, for 18 h. (*D*) Characterization of the 13D10-H11 mAb. 13D10-H11 was tested for cell-surface staining of the reporter cells (*Upper*) and Western blot analysis of the lysate of the reporter cells (*Lower*). Although the control anti-Mincle mAb, IMG-6782, detected Mincle protein in both assays, the 13D10-H11 mAb could only detect

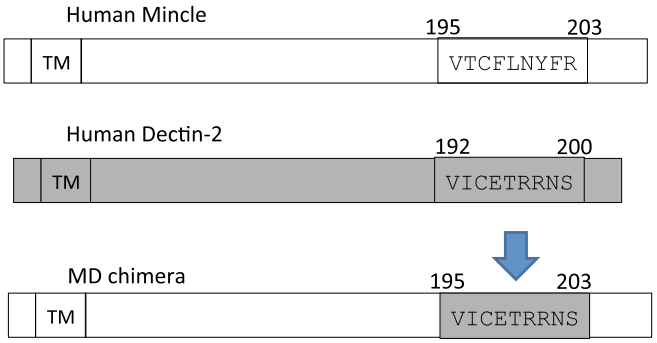

Fig. S4. Schematic representation of the Mincle–Dectin-2 (MD) chimera. The hydrophobic loop in Mincle was mutated to the corresponding amino acid residues in Dectin-2. TM, transmembrane domain.

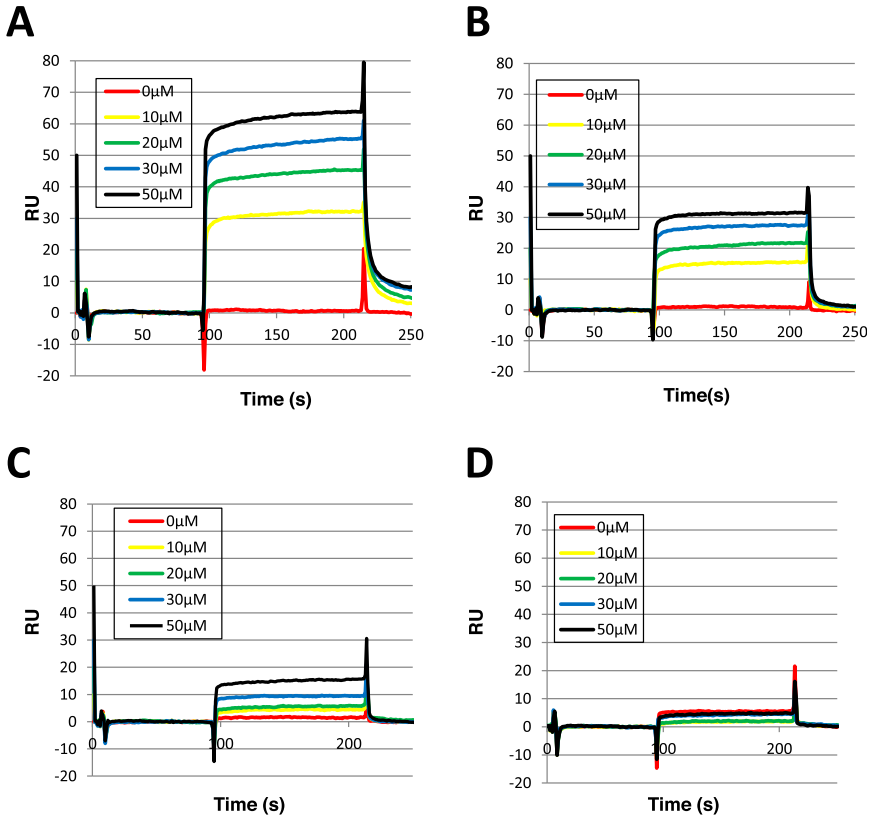

Fig. S5. Surface plasmon resonance (SPR) analysis of Mincle and several lengths of acyl chains with trehalose was performed. Sensorgrams for binding to C12 (*A*), C10 (*B*), C8 (*C*), and trehalose (*D*) in Fig. 4*G* are shown. RU, response units.

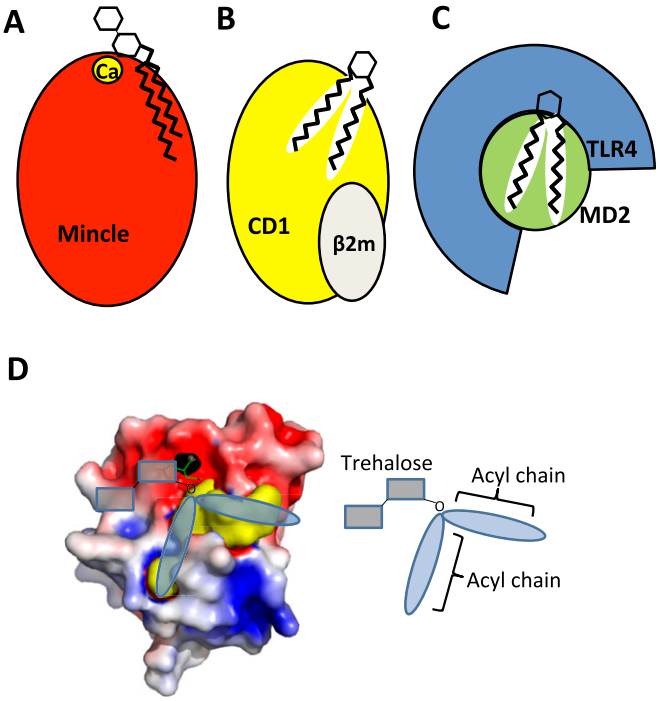

Fig. S6. Schematic images of receptor-recognition mechanisms of glycolipids. (*A*) Mincle. (*B*) CD1d-β2m. (*C*) Toll-like receptor (TLR)4-MD2. (*D*) A modeling image of Mincle with a glycolipid (gray-shaded boxes and blue-shaded circles indicate sugar moieties and acyl chains, respectively).

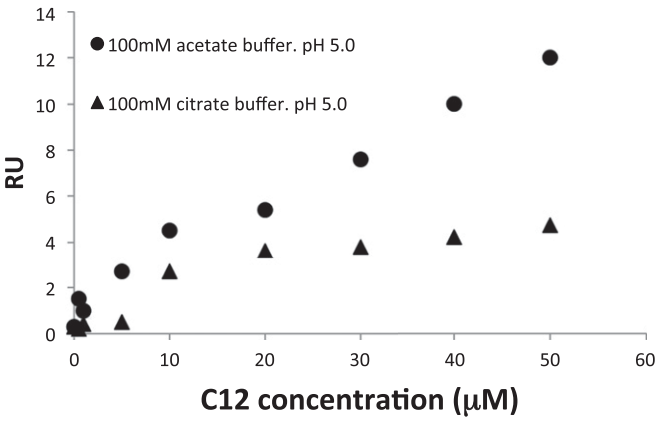

Fig. S7. Competition of Mincle binding to glycolipids with citric acid. SPR analysis of Mincle binding to C12 glycolipid with citric acid (triangles) or acetic acid (circles) was performed.

Table S1. Crystallographic statistics for Mincle and MCL

	Mincle–citrate	Mincle	MCL
Data collection			
Wavelength (Å)	1.000	1.000	1.000
Space group	$P3_1$	$P3_1$	$I222$
Unit-cell parameters (Å)	$a = b = 49.21$, $c = 43.55$	$a = b = 49.07$, $c = 43.04$	$a = 85.19$, $b = 96.06$, $c = 104.83$
Resolution range (Å)	19.39–1.30 (1.35–1.30)	24.54–1.32 (1.37–1.32)	40.48–2.29 (2.372–2.29)
Total no. of observations	158,974	145,199	141,555
Unique reflections	29,014 (2,892)	27,209 (2,690)	19,569 (1,784)
Redundancy	5.5 (5.0)	5.3 (3.5)	7.2 (7.1)
Completeness (%)	99.9 (99.3)	99.9 (98.5)	99.2 (92.1)
Mean I/σ (I)	23.0 (3.1)	17.7 (3.3)	8.65 (3.92)
R_{merge}	0.078 (0.518)	0.070 (0.298)	0.141 (0.496)
Refinement			
R_{work}/R_{free}	0.128/0.156 (0.165/0.206)	0.137/0.171 (0.298/0.318)	0.176/0.218 (0.217/0.234)
No. of atoms			
Protein	1,090	1,060	2,426
Ligand/ion	15	2	2
Water	175	165	231
Average B factors			
Protein	8.6	12.6	34.7
Ligand/ion	14.7	13.5	30.1
Water	21.9	26.8	36.5
Rms deviations			
Bond lengths (Å)	0.005	0.006	0.009
Bond angles (°)	1.12	1.13	1.17
Ramachandran favored/outliers (%)	98/0	97/0	98/0

Numbers in parentheses represent the value of outermost shell.